Inorg. Chem. **2007**, *46*, 7326–7340

MO Tripeptide Diastereomers (M = $^{99/99m}$Tc, Re): Models To Identify the Structure of ^{99m}Tc Peptide Targeted Radiopharmaceuticals

Melchor V. Cantorias,[†] Robertha C. Howell,[†] Louis Todaro,[†] John E. Cyr,[‡] Dietmar Berndorff,[‡] Robin D. Rogers,[§] and Lynn C. Francesconi*,[†]

Department of Chemistry, Hunter College and the Graduate Center of the City University of New York, 695 Park Avenue, New York, New York 10021, Research Laboratories of Schering AG, Radiopharmaceuticals Research, Berlin, Germany, and Department of Chemistry, University of Alabama, Tuscaloosa, Alabama 35487

Received January 16, 2007

Biologically active molecules, such as many peptides, serve as targeting vectors for radiopharmaceuticals based on ^{99m}Tc. Tripeptides can be suitable chelates and are easily and conveniently synthesized and linked to peptide targeting vectors through solid-phase peptide synthesis and form stable $Tc^{V}O$ complexes. Upon complexation with $[TcO]^{3+}$, two products form; these are syn and anti diastereomers, and they often have different biological behavior. This is the case with the approved radiopharmaceutical [^{99m}TcO]depreotide ([^{99m}TcO]P829, NeoTect) that is used to image lung cancer. [^{99m}TcO]depreotide indeed exhibits two product peaks in its HPLC profile, but assignment of the product peaks to the diastereomers has proven to be difficult because the metal peptide complex is difficult to crystallize for structural analysis. In this study, we isolated diastereomers of [^{99}TcO] and [ReO] complexes of several tripeptide ligands that model the metal chelator region of [^{99m}TcO]depreotide. Using X-ray crystallography, we observed that the early eluting peak (A) corresponds to the anti diastereomer, where the Tc═O group is on the opposite side of the plane formed by the ligand backbone relative to the pendant groups of the tripeptide ligand, and the later eluting peak (B) corresponds to the syn diastereomer, where the Tc═O group is on the same side of the plane as the residues of the tripeptide. ^{1}H NMR and circular dichroism (CD) spectroscopy report on the metal environment and prove to be diagnostic for syn or anti diastereomers, and we identified characteristic features from these techniques that can be used to assign the diastereomer profile in ^{99m}Tc peptide radiopharmaceuticals like [^{99m}TcO]depreotide and in ^{188}Re peptide radiotherapeutic agents. Crystallography, potentiometric titration, and NMR results presented insights into the chemistry occurring under physiological conditions. The tripeptide complexes where lysine is the second amino acid crystallized in a deprotonated metallo-amide form, possessing a short N_1–M bond. The pK_a measurements of the N_1 amine (p*K*a ~5.6) suggested that this amine is rendered more acidic by both metal complexation and the presence of the lysine residue. Furthermore, peptide chelators incorporating a lysine (like the chelator of [TcO]depreotide) likely exist in the deprotonated form in vivo, comprising a neutral metal center. Deprotonation possibly mediates the interconversion process between the syn and anti diastereomers. The N_1 amine group on non-lysine-containing metallopeptides is not as acidic (pK_a ~6.8) and does not deprotonate and crystallize as do the metallo-amide species. Three of the tripeptide ligands (FGC, FSC, and FKC) were radiolabeled with ^{99m}Tc, and the individual syn and anti isomers were isolated for biodistribution studies in normal female nude mice. The main organs of uptake were the liver, intestines, and kidneys, with the FGC compounds exhibiting the highest liver uptake. In comparing the diastereomers, the syn compounds had substantially higher organ uptake and slower blood clearance than the anti compounds.

Introduction

Technetium-99m, ^{99m}Tc, is used in over 85% of single photon emission computed tomography (SPECT) scans.[1−3] The prevalence of ^{99m}Tc in nuclear medicine is due to its excellent physical properties (γ ray = 142 keV, half-life = 6.02 h) and its good availability; $^{99m}TcO_4^-$ is conveniently

* To whom correspondence should be addressed. E-mail: lfrances@hunter.cuny.edu, Phone: 212-772-5353, Fax: 212-772-5332.
[†] Hunter College and the Graduate Center of the City University of New York.
[‡] Research Laboratories of Schering AG.
[§] University of Alabama.

(1) Jurisson, S.; Berning, D.; Jia, W.; Ma, D. *Chem. Rev.* **1993**, *93*, 1137−1156.
(2) Chen, J.; Giblin, M.; Wang, N.; Jurisson, S. S.; Quinn, T. P. *Nucl. Med. Biol.* **1999**, *26*, 687−693.
(3) Mahmood, A.; Jones, A. G. In *Handbook of Radiopharmaceuticals*; Welch, M. J., Redvanly, C. S., Eds.; John Wiley and Sons, Ltd.: West Sussex, U.K., 2003; pp 323−362.

10.1021/ic070077p CCC: $37.00
Published on Web 08/11/2007

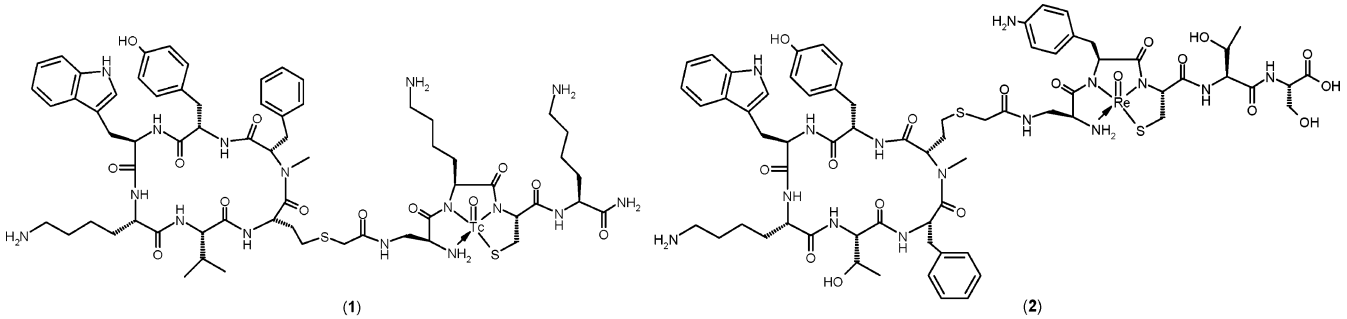

Figure 1. The structures of [TcO] depreotide and [ReO]P2045.

obtained from a ^{99}Mo → ^{99m}Tc generator. The γ ray from ^{99m}Tc penetrates the body, and the energy renders optimal imaging with current gamma camera technology. The relatively short half-life insures that the radiopharmaceutical can be prepared, injected into the patient, and imaging can be accomplished with minimal radiation burden to the patient. Moreover, ^{99m}Tc decays to ^{99}Tc, a very weak β^- emitter, that provides no interference or degradation of image quality.

Whereas most clinically used ^{99m}Tc imaging agents are small coordination compounds that distribute in the body according to their size, charge, and hydrophilicity, recent research has focused on the discovery and development of specifically targeted Tc bioconjugate molecules, which distribute in the body according to a targeting vector, for example an antibody targeted toward an antigen at a tumor site or a peptide or small molecule targeted toward a receptor. The targeting vector is typically connected via a linker to an organic ligand that forms a coordination complex with the metal ion, called a metal chelate. The organic ligand and the linker are often called a bifunctional chelate (BFC).

The first, and thus far only, specifically targeted ^{99m}Tc radiopharmaceuticals that are approved and in clinical use are based on cyclic peptide targeting vectors that are linked to tripeptide ligand motifs. The first ^{99m}Tc radiopharmaceutical of this type to be introduced to the clinic was [^{99m}TcO]-apcitide (^{99m}Tc P246, AcuTect), the technetium complex of the 13 amino acid peptide, apcitide, cyclo-[D-Tyr-Apc-Gly-Asp-Cys]-Gly-Gly-Cys(Acm)-Gly-Cys(Acm)-Gly-Gly-Cys-NH_2. [^{99m}TcO]apcitide has high affinity and selectivity for the GPIIb/IIIa receptor[4,5] and is used for imaging acute DVT. One complex forms in this radiopharmaceutical preparation, where the ^{99m}Tc is coordinated to the C-terminal Gly-Gly-Cys sequence of apcitide.[6] The chelation about the technetium is denoted as N_3S because the coordinating atoms in the peptide include three nitrogens (three amide nitrogen atoms of Gly, Gly, and Cys) and one sulfur (the thiol sulfur of Cys).

The second ^{99m}Tc-labeled peptide to receive regulatory approval is [^{99m}TcO]depreotide (^{99m}Tc P829, NeoTect) for lung tumor imaging. [TcO]depreotide (**1**, Figure 1) is comprised of a cyclic hexapeptide containing a somatostatin receptor (SSTR) binding sequence and a linear tetrapeptide, which forms a coordination complex with technetium at the Dap-Lys-Cys sequence (Dap = β-diaminopropioninc acid). Chelation about the technetium in [TcO]depreotide is also N_3S because the coordinating atoms in the peptide include three nitrogens (two amide nitrogen atoms of Lys and Cys and one amine nitrogen of Dap) and one sulfur (the thiol sulfur of Cys). Another radiolabeled SSTR binding peptide with an N_3S peptide chelator similar to that of [^{99m}TcO]-depreotide is the radiotherapy agent [^{188}ReO]P2045 (**2**, Figure 1) (NeoTide).[7] On the basis of previous results for technetium(V) and rhenium(V) complexes of peptide-based ligands of the N_3S type,[8,9] the [TcO]depreotide and [ReO]P2045 complexes are expected to have a distorted square pyramidal structure, with the oxo group perpendicular to the plane of the peptide nitrogen and sulfur coordinating atoms.

When peptide-based chelators are comprised of amino acids containing side chains, chiral centers are incorporated into the coordination plane, and diastereomeric complexes are known to form where the M═O group (M = Tc, Re) is either syn or anti to the substituents.[9−15] The two possible diastereomers for the Dap-X-Cys type of peptide chelator found on [TcO]depreotide and [ReO]P2045 are depicted in Figure 2. For discussion here, the two diastereomers will be

(4) Lister-James, J.; Knight, L. C.; Maurer, A. H.; Bush, L. R.; Moyer, B. R.; Dean, R. T. *J. Nucl. Med.* **1996**, *37*, 775.
(5) Lister-James, J.; Dean, R. T. In *Technetium, Rhenium and Other Metals in Chemistry and Nuclear Medicine*; Nicolini, M., Mazzi, U., Eds.; Servizi Grafici Editoriali: Padova, Italy, 1999; pp 401−407.
(6) Francesconi, L. C.; Zheng, Y.; Bartis, J.; Blumenstein, M.; Costello, C.; DeRosch, M. *Inorg. Chem.* **2004**, *43*, 2867−2875.
(7) Cyr, J. E.; Wilson, D. W.; Nelson, C. E.; Lister-James, J.; Dean, R. T.; Dinkelborg, L. M.; Pearson, D. A. *J. Med. Chem.* **2007**, *50*, 1354−1364.
(8) Grummon, G.; Rajagopalan, R.; Palenik, G.; Koziol, A.; Nosco, D. *Inorg. Chem.* **1995**, *34*, 1764−1772.
(9) Wong, E.; Fauconnier, T.; Bennett, S.; Valliant, J.; Nguyen, T.; Lau, F.; Lu, L.; Pollak, A.; Bell, R.; Thornback, J. *Inorg. Chem.* **1997**, *36*, 5700−5708.
(10) Bormans, G.; Cleynhens, B.; Adriaens, P.; De Roo, M.; Verbruggen, A. *J. Labelled Compd. Radiopharm.* **1993**, *33*, 1065−1078.
(11) Epps, L. A.; Burns, H. D.; Lever, S. Z.; Goldfarb, H. W.; Wagner, H. N. *Appl. Radiat. Isot.* **1987**, *38*, 661−664.
(12) Baidoo, K. E.; Lever, S. Z. *Bioconjugate Chem.* **1990**, *1*, 132−137.
(13) Cyr, J. E.; Nowotnik, D. P.; Pan, Y.; Gougoutas, J. Z.; Malley, M. F.; DiMarco, J.; Nunn, A. D.; Linder, K. E. *Inorg. Chem.* **2001**, *40*, 3555−3561.
(14) Luyt, L. G.; Jenkins, H. A.; Hunter, D. H. *Bioconjugate Chem.* **1999**, *10*, 470−479.
(15) Rao, T. N.; Adhikesavalu, D.; Camerman, A.; Fritzberg, A. R. *J. Am. Chem. Soc.* **1990**, *112*, 5798−5804.

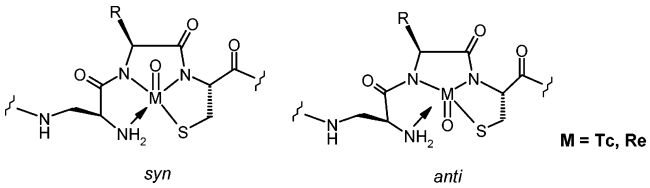

Figure 2. Peptide-based metal binding N_3S chelator Dap-X-Cys typical of [TcO]depreotide and [ReO]P2045, depicting possible syn and anti isomers (syn and anti relative to the R side chain).

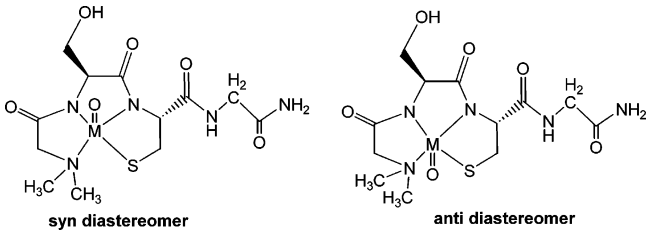

Figure 3. The syn and anti diastereomers of [MO] RP294 (M = Tc, Re; RP294 = dimethylglycine-serine-cysteine-glycine.)

referred to as syn or anti with regard to the position of the side chain on the second amino acid (X) relative to the M═O bond.

It is well established that stereoisomers of radiopharmaceutical products can have distinctly different biodistributions. For example, the meso isomer of HMPAO (the brain perfusion radiopharmaceutical Ceretec) yields a ^{99m}Tc complex with lower brain uptake than that of the D,L-HMPAO isomer.[16] Considering another brain agent (Neurolite), the ^{99m}Tc complex of L,L-ECD is metabolized in the brain and retained, whereas ^{99m}Tc D,D-ECD is not metabolized and washes out quickly.[17] Isolated syn/anti pairs of Tc(V) complexes have also shown different biodistribution profiles.[15,18−22] In cases where radiopharmaceuticals can form two distinct isomeric species, it is important to evaluate the individual products separately to ensure that they both possess good biological efficacy. Identification of the structures of these diastereomers is also very important, especially as it relates to understanding structure−activity aspects of biological behavior and to identifying the fundamental issues governing the stability of diastereomers and diastereomer distribution.

Two main products are indeed formed when depreotide peptide is radiolabeled with ^{99m}Tc, and these are purported to be the syn and anti diastereomers of [TcO]depreotide. In [^{99m}TcO]depreotide, the early eluting peak, labeled A was found in ca. 10% radiochemical yield and the later eluting peak B was 90% yield. The [^{99m}TcO]depreotide diastereomers exhibited different biological properties, although both have nanomolar affinities for the somatostatin receptor.[23] We set out to try to assign the two diastereomers of [^{99m}TcO]-depreotide through X-ray structural characterization but were unsuccessful because suitable X-ray quality crystals were not obtained. Intermediate size peptides such as depreotide (or P2045) and their metal complexes are difficult to crystallize as compared to smaller compounds.

As an alternative approach, we chose to investigate tripeptide complexes of ^{99}Tc that model the metal chelate shown in Figure 2 as crystallographic standards (i.e., smaller peptide complexes that crystallized more readily). NMR and circular dichroism (CD) spectroscopy were evaluated as probes for characterizing the metal centers of the syn versus anti species. As a result, spectroscopic benchmarks were identified to assign syn and anti diastereomers of ^{99m}Tc and ^{188}Re peptide chelates. The NMR and CD techniques were suitable for assigning the syn/anti diastereomers of [^{99m}TcO]-depreotide (details of the [^{99m}TcO]depreotide characterization and biological characterization are reported elsewhere).[23] Furthermore, the NMR and CD methods thus defined would be useful for assigning syn versus anti diastereomers in a variety of other targeted ^{99m}Tc/^{188}Re radiopharmaceuticals regardless of the targeting vector because they directly report on the environment about the metal center.

We chose tripeptide ligands (X_1-X_2-Cys-NH_2; X_1 = Phe, Met, Tyr, or ϵ-benzoyl-Lys; X_2 = Gly, Lys, Ser, or Asp) that do not undergo interconversion appreciably so that the diastereomers could be isolated, crystallized, and characterized. Rapid interconversion has precluded previous attempts to identify specific diastereomers of Tc peptide complexes and to correlate these with HPLC profiles.[9,24] RP 294, $(Me)_2$-Gly-Ser-Cys(Acm)-Gly-NH_2, a hydrophilic, unencumbered peptide ligand that binds technetium and rhenium, forms diastereomers that rapidly interconvert and cannot be individually isolated (Figure 3). ^{1}H NMR and ^{13}C NMR confirmed that the ^{99}Tc and Re products of RP 294 are diastereomers, and indeed, a crystal structure showing the syn diastereomer was solved. However, the crystal was isolated from a mixture of syn and anti diastereomers (as shown by NMR and HPLC), and rapid interconversion precluded clean isolation and correlation with the HPLC profile. The RP 294 tripeptide motif has been appended onto targeting vectors using solid-phase synthetic methodology and specific diastereomeric distinction similarly was not achieved.[25−29]

(16) Sharp, P. F.; Smith, F. W.; Gemmell, H. G.; Lyall, D.; Evans, N. T. S.; Gvozdanovic, D.; Davidson, J.; Tyrrell, D. A.; Pickett, R. D.; Neirinckx, R. D. *J. Nucl. Med.* **1986**, *27*, 171−177.
(17) Walovitch, R. C.; Makuch, J.; Knapik, G.; Watson, A. D.; Williams, S. J. *J. Nucl. Med.* **1988**, *29*, 747 (abstr).
(18) Bormans, G.; Cleynhens, B.; José, D.; Hoogmartens, M.; De Roo, M.; Verbruggen, A. *Nucl. Med. Biol.* **1990**, *17*, 499−506.
(19) Francesconi, L. C.; Graczyk, G.; Wehrli, S.; Shaikh, S.; McClinton, D.; Liu, S.; Zubieta, J.; Kung, H. *Inorg. Chem.* **1993**, *32*, 3114−3124.
(20) Kung, H.; Guo, Y.; Yu, C.; Billings, J.; Subramanyam, V.; Calabrese, J. *J. Med. Chem.* **1989**, *32*, 433−437.
(21) Lever, S. Z.; Burns, H. D.; Kervitsky, T. M.; Goldfarb, H. W.; Woo, D. V.; Wong, D. F.; Epps, L. A.; Kramer, A. V.; Wagner, H. N. *J. Nucl. Med.* **1985**, *26*, 1287−1294.
(22) Meegalla, S. K.; Plossl, K.; Kung, M. P.; Chumpradit, S.; Stevenson, D. A.; Kushner, S. A.; McElgin, W. T.; Mozley, P. D.; Kung, H. F. *J. Med. Chem.* **1997**, *40*, 9−17.
(23) Cyr, J. E.; Pearson, D. A.; Nelson, C. A.; Lyons, B. A.; Zheng, Y.; Bartis, J.; He, J.; Cantorias, M.; Howell, R.; Francesconi, L. C. *J. Med. Chem.* **2007**, in press.
(24) Valliant, J. F.; Riddoch, R. W.; Hughes, D. W.; Roe, D. G.; Fauconnier, T. K.; Thornback, J. R. *Inorg. Chim. Acta* **2001**, *325*, 155−163.
(25) Caveliers, V.; Goodbody, A. E.; Tran, L. L.; Peers, S. H.; Thornback, J. R.; Bossuyt, A. *J. Nucl. Med.* **2001**, *42*, 154−161.
(26) Wong, E.; Bennett, S.; Lawrence, B.; Fauconnier, T.; Lu, L. F. L.; Bell, R. A.; Thornback, J. R.; Eshima, D. *Inorg. Chem.* **2001**, *40*, 5695−5700.
(27) van de Wiele, C.; Dumont, F.; Dierckx, R. A.; Peers, S. H.; Thornback, J. R.; Slegers, G.; Thierens, H. *J. Nucl. Med.* **2001**, *42*, 1722−1727.

Rhenium analogs of the tripeptide complexes were also evaluated. Rhenium is the third-row transition-metal congener of Tc and usually exhibits similar complexation chemistry to technetium. Therefore, it is frequently used as a nonradioactive surrogate for characterization of ^{99m}Tc radiopharmaceuticals. Rhenium is also becoming increasingly more important in the field of radiopharmaceuticals as a radiotherapeutic isotope. ^{188}Re has excellent properties for radiotherapy; ^{188}Re (half-life of 16 h) emits a high-energy β^- (E_{max} = 2.11 MeV) with a range of ~3 mm that is effective for cell killing and also generates an imageable γ ray of 155 keV (15%) that can be useful for tracking the radiotherapeutic agent. Just as the availability of the ^{99}Mo → ^{99m}Tc generator drove the research to develop ^{99m}Tc radiopharmaceuticals, the recent availability of the ^{188}W → ^{188}Re generator[30−33] is driving research to develop ^{188}Re radiotherapeutic agents.[34−36] The potential pairing of ^{99m}Tc and ^{188}Re for dosimetry and for targeted radiotherapy, respectively, is an attractive concept.

The goals of this project were (1) to synthesize and structurally characterize the syn and anti diastereomers of Tc/Re complexes of small tripeptide ligands, (2) to identify spectroscopic methods for differentiating between syn versus anti Tc/Re peptide complexes that would be suitable for larger peptide radiopharmaceuticals like [TcO]depreotide, and (3) to assess the biological properties of separated, structurally characterized syn and anti [^{99m}TcO]tripeptide diastereomers.

Experimental Section

General Procedure. Materials. Fmoc-protected L-amino acids and Rink amide MBHA resin were purchased from NovaBiochem. *N*-hydroxybenzotriazole (HBTU) was purchased from ChemTech. 2-(1H-benzotriazole-1-yl)1,1,3-tetramethyluronium (HOBt), *N*,*N*-diisopropylethylamine (DIPEA), piperidine, phenol, thioanisole, triisopropylsilane (TIS), and 1,2-ethanedithiol (EDT) were purchased from Sigma-Aldrich. HPLC-grade acetonitrile, trifluoroacetic acid (TFA), and *N*,*N*-dimethylformamide (DMF) were purchased from Fisher Scientific. Nanopure water was obtained from a Millipore filtration system equipped with a 0.22 μm filter. All of the chemicals were used as received without further purification. The ϵ-benzoyl-Lys-Gly-Cys peptide was synthesized at Diatide, Inc., Londonderry, New Hampshire.

^{99}Tc is a low-energy (0.292 MeV) β^- emitter with a half-life of 2.12×10^5 years. This isotope should be handled in a fume hood using appropriate radioactive protocols. $NH_4{}^{99}TcO_4$ was obtained from Oak Ridge National Laboratory, Oak Ridge, TN. H_2O_2 (30%) was added to an aqueous solution of $NH_4{}^{99}TcO_4$ to oxidize any $^{99}TcO_2$ present. The ammonium pertechnetate solution was standardized prior to use as previously described.[37] The reagent $[TcOCl_4]N(C_4H_9)_4$ was prepared following a published procedure.[38] $N(C_4H_9)_4$ $[ReOBr_4(OP(C_4H_9)_3]$ was prepared according to a published procedure.[39] ^{99m}Tc-pertechnetate (^{99}Mo/^{99m}Tc generator) was obtained from Cardinal Health (Bronx, NY). Na[^{99}TcO-(ethyleneglycol)$_2$] was prepared according to published procedures.[40]

Instrumentation and Analytical Methods. A RAININ Dynamax HPLC system equipped with a Dynamax UV-1 UV−visible detector and two Dynamax model SD-200 pumps using 25 mL pump heads was employed. All of the HPLC experiments were monitored at a λ = 220 nm. A home-built detector composed of Tennelec Minibin components, such as the power supply, high voltage supply, and amplifier, was interfaced to the HPLC system to monitor the γ emissions of ^{99m}Tc. For both analytical and preparative work, the mobile phase consisted of (A) 0.1% TFA in H_2O and (B) acetonitrile. For analytical HPLC, two methods were used: Method 1 − Column: Waters DeltaPak 5μ C_{18} 100 Å, 3.9 × 150 mm; Mobile Phase Gradient: 0−55% B over 30 min; Flow Rate: 1.0 mL/min; Software: Dynamax HPLC Method Manager; Method 2 − Column: Waters XTerra 5μ C_{18} 100 Å, 3.9 × 150 mm; Mobile Phase Gradient: 0−55% B over 15 min; Flow Rate: 1.0 mL/min; Software: ProStar WorkStation. For preparative work, Method 3 consisted of Waters DeltaPak 5μ C_{18} 300 Å, 19.0 × 300 mm column and the software used was Dynamax HPLC Method Manager; the mobile phase gradient was 0−55% B over 30 min at a flow rate of 24 mL/min. The ^{99m}Tc tripeptide diastereomer samples for biodistribution evaluation were separated by Method 4 preparative HPLC using a Zorbax Bonus RP 5μ C_{18}, 4.6 × 250 mm column; the mobile phase consisted of (A) water and (B) ethanol, with varying gradients over 20 min at a flow rate of 1.0 mL/min as follows: ^{99m}Tc FGC = 25−55% B; ^{99m}Tc FSC = 15−40% B; ^{99m}Tc FKC = 10−50% B. Analytical HPLC runs for the isolated diastereomers for ^{99m}Tc biology samples utilized (Method 5) the same HPLC column but a different mobile phase: (A) 0.1% TFA in water and (B) 0.1% TFA in 90:10 acetonitrile:water. Method 5 analytical gradients (or isocratic conditions as noted) were also over 20 min at a flow rate of 1.0 mL/min as follows: ^{99m}Tc FGC = 15−50% B; ^{99m}Tc FSC = 25% B isocratic; ^{99m}Tc FKC = 15−35% B.

Mass spectral data was acquired, for Re compounds, on an Agilent Technologies 1100 Series LC/MS model G1946D using electrospray ionization in the positive-ion mode. The ^{99}Tc compounds were analyzed at the University of Illinois Mass Spectrometry Center. Infrared spectra were recorded from KBr disks on a Perkin-Elmer 1600 FT-IR spectrometer in the range of 600−3000 nm and were referenced to polystyrene film. Proton NMR spectra

(28) *Rhenium and Technetium-99m Oxocomplexes of Neurotensin*; Chavatte, K., Wong, E., Fauconnier, T. K., Lu, L., Nguyen, T., Roe, D., Pollak, A., Eshima, D., Terriere, D., Mertens, J., Herbeke, K., Tourwe, D., Thornback, J., Bossuyt, A., Eds.; SGE Editoriali: Padova, Italy, 1999; Vol. 5.
(29) Zhang, X.; Su, Z.-F.; Ballinger, J. R.; Rauth, A. M.; Pollak, A.; Thornback, J. R. *Bioconjugate Chem.* **2000**, *11*, 401−407.
(30) Knapp, F. F.; Beets, A. L.; Guhlke, S.; Zamora, P. O.; Bender, H.; Palmedo, H.; Biersack, H. J. *Anticancer Res.* **1997**, *17*, 1783.
(31) Guhlke, S.; Beets, A. L.; Oetjen, K.; Sartor, J.; Mirzadeh, S.; Knapp, F. F.; Biersack, H. J. *J. Labelled Compd. Radiopharm.* **1997**, *39*, 294.
(32) Ehrhardt, G.; Ketring, A. R.; Turpin, T. A.; Razavi, M. S.; Vanderheyden, J. L.; Fritzberg, A. R. *J. Nucl. Med.* **1987**, *28*, 656−657.
(33) Ehrhardt, G.; Ketring, A.; Liang, Q. *Radioact. Radiochem.* **1992**, *3*, 38−41.
(34) Dadachova, E.; Moadel, T.; Schweitzer, A. D.; Bryan, R. A.; Zhang, T.; Mints, L.; Revskaya, E.; Huang, X.; Ortiz, G.; Nosanchuk, J. S.; Nosanchuk, J. D.; Casadevall, A. *Cancer Biother. Radiopharm.* **2006**, *21*, 1−13.
(35) Dadachova, E.; Nosanchuk, J. D.; Shi, L.; Casadevall, A. *Proc. Natl. Acad. Sci. U.S.A.* **2004**, *101*, 14865−14870.
(36) Dadachova, E.; Patel, M. C.; Toussi, S.; Apostolidis, C.; Morgenstern, A.; Brechbiel, M. W.; Gorny, M. K.; Zolla-Pazner, S.; Casadevall, A.; Goldstein, H. *PLoS Medicine* [Online] **2006**, *3*, 2094−2103.
(37) Boyd, G. *J. Chem. Educ.* **1959**, *36*, 3.
(38) Davison, A.; Trop, H.; DePamphilis, B.; Jones, A. *Inorg. Synth.* **1982**, *21*, 160.
(39) Rose, D. J.; Maresca, K. P.; Kettler, P. B.; Chang, Y. D; Soghomomian, V.; Chen, Q.; Abrams, M. J.; Larsen, S. K.; Zubieta, J. *Inorg. Chem.* **1996**, *35*, 3548−3558.
(40) DePamphilis, B. V.; Jones, A. G.; Davison, A. *Inorg. Chem.* **1983**, *22*, 2292−2297.

Table 1. Selected Bond Lengths (Angstroms) and Bond Angles (Degrees) for MO Tripeptide Diastereomers (M = ^{99}Tc, Re)

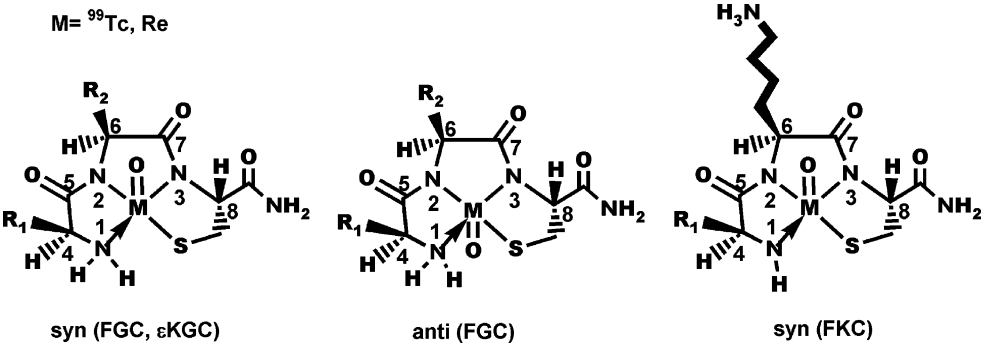

bond length (Å)	[TcO]FGC anti	[ReO]FGC anti	[ReO]FGC syn	[TcO](ϵK)GC syn	[ReO]FKC syn
M−O	1.678(5)	1.682(7)	1.659(2)	1.664(3)	1.690(3)
M−S	2.2828(17)	2.256(2)	2.2588(10)	2.2814(14)	2.2975(12)
M−N1	2.103(5)	2.116(7)	2.129(3)	2.111(4)	1.931(9)
M−N2	1.980(5)	1.992(7)	1.968(3)	1.980(4)	2.005(4)
M−N3	1.965(5)	1.987(7)	1.985(3)	1.987(4)	2.004(3)
N1−C4	1.479(13)	1.483(10)	1.480(5)	1.511(6)	1.464(6)
bond angle (deg)					
N1−M−N2	77.5(4)	77.6(3)	77.75(12)	76.93(16)	77.98(16)
N1−M−S	92.8(2)	89.5(2)	88.68(8)	88.53(12)	91.08(12)
N2−M−N3	79.3(2)	79.0(3)	78.96(12)	78.15(16)	77.13(15)
N3−M−S	82.46(15)	82.6(2)	82.75(8)	82.69(12)	81.93(11)
O−M−N1	107.8(4)	107.4(3)	107.90(13)	114.76(16)	112.07(15)
O−M−N2	112.4(2)	117.0(3)	116.49(12)	113.39(18)	111.39(15)
O−M−N3	110.4(2)	110.3(3)	110.72(12)	113.63(17)	115.48(14)
O−M−S	111.07(16)	113.0(2)	113.26(9)	108.64(13)	109.10(12)
C5−N−C6	121.2(6)	120.0(7)	119.1(3)	120.5(4)	121.3(4)
C7−N3−C8	115.1(5)	117.3(8)	118.4(3)	115.9(4)	116.1(3)
C5−N2−M	121.8(5)	121.7(6)	122.0(3)	121.0(3)	119.8(3)
C6−N2−M	117.0(4)	117.8(5)	118.1(2)	118.4(3)	118.0(3)
C7−N3−M	118.6(4)	120.0(6)	119.5(3)	119.6(3)	118.6(3)
C8−N3−M	124.6(4)	122.2(6)	121.6(2)	123.1(3)	125.2(3)
C4−N1−M	111.7(5)	112.0(5)	111.1(2)	111.0(3)	119.5(3)
C5−C4−N1	109.6(6)	108.4(7)	108.0(3)	107.7(4)	105.9(4)

Table 2. Deviations (Angstroms) from the Square Plane Formed by the Amine and Amide Nitrogen Atoms and the Thiolate Sulfur Atom

	[TcO]FGC anti	[ReO]FGC anti	[ReO]FGC syn	[TcO](ϵK)GC syn	[ReO]FKC syn
S	0.0861	0.0980	−0.0486	0.0321	−0.0239
N1 (amine)	−0.0955	−0.1083	0.0536	−0.0356	0.0269
N2 (amide)	0.1159	0.1311	−0.0669	0.0431	−0.0320
N3 (amide)	−0.1065	−0.1208	0.0619	−0.0396	0.0289

including TOCSY (total correlation spectroscopy), NOESY (nuclear Overhauser effect spectroscopy), as well as COSY (correlation spectroscopy) were recorded on a Varian Inova 500 MHz NMR spectrometer at $T = 296$ K. The chemical shift was referenced to H_2O as an internal reference. Circular Dichroism (CD) spectra of methanolic solutions of the ^{99}Tc and Re tripeptides were collected on a JASCO-J710 spectropolarimeter where the optical system was fed by a prepurified nitrogen compressed gas at a flow rate of 5 L/min.

X-ray Crystallography. Small rodlike crystals of ^{99}Tc/Re tripeptides were isolated from solution and examined under a thin layer of mineral oil using a polarizing microscope. A suitable crystal was chosen and mounted on a glass fiber while still coated in oil; the crystal was then immediately frozen to 100 K on a Bruker Nonius Kappa CCD diffractometer equipped with a sealed-tube Mo anode (Kα radiation, $\lambda = 0.71073$ Å) and a graphite monochromator. Data collection, indexing, and initial cell refinements were all handled using accompanying proprietary Nonius software. A yellow single crystal of the ^{99}Tc ϵ-benzoyl-Lys-Gly-Cys syn diastereomer was mounted on a fiber, transferred to the goniometer, cooled to −100 °C, and data was collected on a Bruker Apex diffractometer. The SHELX package of software was used to solve and refine structures. The heaviest atoms were located by direct methods, and the remaining atoms were found in a subsequent Fourier difference. A disordered ethanol molecule was found in one structure of ReO FKC, crystallized from ethanol/methylene chloride. The crystal and structure refinement data for selected ^{99}Tc and Re tripeptide diastereomers are given in Table S1, selected bond lengths and angles are listed in Table 1, and deviations of the amine and amide nitrogen atoms and the thiolate sulfur from the square plane constructed from these atoms are listed in Table 2. The crystal structure refinement data and bond lengths and angles for two additional complexes, [ReO] FKC syn, crystallized from a basic aqueous solution, and [TcO] YKC syn, crystallized from an organic solution, are given in Tables S2 and S3, respectively, in the Supporting Information. The structure of [TcO] YKC syn showed three molecules in the unit cell, two of which were disordered. Ortep diagrams of all of the molecules are presented in Figure S1, Supporting Information.

Preparation of Complexes. General Procedure for Preparation of Tripeptide Ligands. Peptides were prepared via solid-phase peptide synthesis on a home-built peptide synthesizer. Fmoc-

protected amino acids and Rink amide MBHA resin were used. Details of the preparation of tripeptides are given in the Supporting Information**.**

The peptides prepared in this study are Phe-Gly-Cys-NH_2 (FGC), Phe-Lys-Cys-NH_2 (FKC), Met-Lys-Cys-NH_2 (MKC), Tyr-Lys-Cys-NH_2 (YKC), Tyr-Ser-Cys-NH_2 (YSC), Tyr-Asp-Cys-NH_2 (YDC), Tyr-Gly-Cys-NH_2 (YGC) and ϵ-benzoyl-Lys-Gly-Cys-NH_2 (ϵ-benzoyl-KGC). The one-letter amino acid code is in the parentheses. Cysteine is always at the C terminus of the tripeptides and is capped as an amide.

General Procedure for Preparation of ^{99}Tc/Re Tripeptides. The following procedures are prototypical preparations for all of the ^{99}Tc and Re tripeptide complexes. Selected NMR data (organic solution) and mass spectral data are shown in Figures S2 and S3, respectively. The HPLC retention times of all of the species and their infrared stretching frequencies and selected mass spectral data are given in Tables S4 and S5, respectively, in the Supporting Information. Full NMR data and CD data are tabulated in Tables S6 and S7, respectively (Supporting Information).

Synthesis of [Re^{V}O]Phe-Gly-Cys. The tripeptide, Phe-Gly-Cys-NH_2 (FGC) (14.6 mg, 0.045 mmol), $N(C_4H_9)_4[ReOBr_4(OP(C_4H_9)_3)]$ (40.3 mg, 0.041 mmol), and sodium acetate (6.15 mg, 0.075 mmol) were dissolved in 2 mL methanol. The resulting mixture became a dark-brown solution instantly and was stirred for 2 min. The crude solution was analyzed on an HPLC system using Method 1 (Instrumental and Analytical Methods, vide supra), showing two major peaks, representing the two diastereomers. The diastereomeric products were then isolated and purified using semipreparative HPLC, Method 3, vide supra. The collected HPLC fractions were lyophilized, yielding a fluffy powder for each product. The early eluting product was dark peach in color and the later eluting product was light peach.

Synthesis of [^{99}Tc^{V}O] Phe-Gly-Cys. $N(C_4H_9)_4[^{99}TcOCl_4]$ (20.5 mg, 0.041 mmol) was dissolved in 2 mL methanol. FGC (14.6 mg, 0.045 mmol) and sodium acetate (6.2 mg, 0.075 mmol) were combined. The methanolic $^{99}TcOCl_4^-$ solution was then added to the peptide/acetate solid mixture. This resulted in a dark-purple solution, which was analyzed on the HPLC using Method 2, vide supra, resulting in two major peaks. Isolation and purification was subsequently accomplished using semipreparative HPLC following Method 3, vide supra. Two distinct colors were observed during fraction collection in solution. The first eluting product was pink in color, and the late eluting product was yellow. The powders that resulted from lyophilization were also pink for the early eluting peak A and yellow for the later eluting peak B.

General Crystallization Procedure for [^{99}TcO]/[ReO]FGC Tripeptide Complexes for X-ray Crystal Structure Experiments. The sample (3 mg) was dissolved in a 2 mL vial with a minimum amount of ethyl acetate or methylene chloride. A few drops of ethanol were added to completely dissolve the sample. The small vial was placed without a cover into a 20 mL vial containing about 5 mL pentane. The larger vial was then capped and allowed to stand at 10 °C. Crystals were formed within days.

Crystallization of [Re^{V}O]Phe-Lys-Cys. Crystals for the diastereomers of [Re^{V}O]Phe-Lys-Cys were grown by two methods. In the first method, the compound was dissolved in 1:1 ethanol/methylene chloride and allowed to slowly evaporate. The second method involved slow evaporation of an aqueous solution of the compound after the addition of 100 μL of 1% NaOH in D_2O. Specifically, ca. 5 mg of the syn compound was dissolved in about 125 μL of water. The color and pH of the resulting solution was dark brown and 3.8, respectively. Sodium hydroxide (1%, 100 μL in D_2O) was immediately added to the solution. The color of the solution turned yellow-brown and the final pH was 13.3. The vial containing this sample was left overnight under the fume hood without cover. Yellow-brown crystals were formed within hours.

Synthesis and Crystallization of [^{99}Tc^{V}O]ϵ-benzoyl-Lys-Gly-Cys. The peptide (9.8 mg, 0.024 mmol) was dissolved in 0.5 mL methanol. To this stirring solution 0.71 mL of a 0.034 mM Na[^{99}-TcO(ethyleneglycol)$_2$] in methanol stock solution was added. The solution immediately turned yellow-brown and was capped and stirred for 5 h. Two fractions were collected by preparative HPLC (32−34 min and 39−42 min). As for the [TcO]Phe-Gly-Cys preparation, the solution containing the first eluting peak was pink, and the late eluting peak solution was yellow. The fractions were lyophilized to form powders. Also, as for other aqueous ^{99}Tc preparations, the powders resulting from the lyophilization were pink for the early eluting peak A and yellow for the later eluting peak B. Crystallization of compound B was achieved by evaporation of a methanol/acetonitrile solution.

Radiolabeling of Tripeptides with ^{99m}Tc. Radiolabeling Method 1. To a 1.5 mL microcentrifuge tube, 25 μL of the tripeptide solution (0.6 mg/mL in saline) and 10 μL of sodium tartrate (50 mg/mL in ammonium buffer that contains 0.5 M $(NH_4)_2CO_3$, 0.25 M $NH_4O_2CCH_3$, and 0.18 M NH_4OH) were added and mixed. In a lead shielded fumehood, the tripeptide/tartrate solution was radiolabeled by adding 100 μL of ^{99m}Tc sodium pertechnetate (500−600 μCi) followed by 5 μL $SnCl_2 \cdot 2H_2O$ (1 mg/mL in 0.01 M HCl). The solution (pH 8) was vortexed briefly. HPLC analyses were performed on samples prepared at room temperature and after heating in a boiling water bath for various durations. HPLC analyses with radiometric detection were generally performed with a ca. 35 μCi sample.

Radiolabeling Method 2. For biodistribution studies, samples of [^{99m}TcO]FGC, [^{99m}TcO]FSC, and [^{99m}TcO]FKC were made by a modified procedure, and the individual diastereomers were isolated by preparative HPLC. Placebo kits were prepared containing all of the components (lyophilized) necessary to radiolabel with ^{99m}Tc except the peptides in a 5 mL vial, stoppered under nitrogen. The placebo kit vials contained 5 mg sodium α-D-glucoheptonate dihydrate, 100 μg edetate disodium (EDTA), and 50 μg tin(II) chloride dihydrate at pH 7.4. Peptides to be radiolabeled were dissolved in 0.01 M HCl at 1 mg/mL, and 75 μg (75 μL) of peptide was added to placebo kits. Vials were reconstituted with 400−700 μL of ^{99m}Tc pertechnetate generator eluate containing 20−25 mCi of $^{99m}TcO_4^-$ and heated for 10 min in a boiling water bath. After cooling the vials at room temperature for ∼10 min, the diastereomeric products were isolated by reverse phase HPLC using Method 4 (vide supra), which employed an ethanol/water gradient mobile phase. The fractions containing the pure ^{99m}Tc diastereomeric products were diluted with saline and used directly for injection into mice. The samples were checked for purity using reverse phase HPLC Method 5 vide supra. All of the final samples had radiochemical purity by HPLC ≥ 90%.

Procedures for Analysis of ^{99}Tc/Re Tripeptide Complexes. NMR Spectroscopy. [^{99}TcO] or [ReO] tripeptide complex (3 mg) was dissolved in 600 μL of 0.01 M HCl. D_2O (60 μL) was then added to the acidified solution. The sample solution was transferred into a 5 mm NMR tube. 1D H NMR spectra were collected at 64 scans. 2D NMR (COSY, TOCSY, and NOESY) were collected at 128 scans for each spectra.

Circular Dichroism Studies. [^{99}TcO]/[ReO] tripeptide complex (1 mg) was dissolved in 1 mL methanol. The aliquot (250 μL) was placed in a 250 μL CD cell. The sample was scanned from 170 to 600 nm with ± 50 degree sensitivity. The CD spectra were collected with baseline and background corrections using pure methanol.

HPLC Coelution Studies. Prepared [^{99}TcO] tripeptide crude mixture (5 μL) was withdrawn into a 25 μL Hamilton syringe. To the same syringe, a volume containing a ca. 35 μCi dose of the analogous ^{99m}Tc tripeptide solution was added. The total volume was injected into the HPLC system. The coelution, monitored by UV for the ^{99}Tc species and radiometric (γ) detection for the tracer ^{99m}Tc species, demonstrated that, under the HPLC conditions, the two species are chemically identical.

Procedure for Simultaneous Potentiometric and NMR Titrations. Standard solutions of NaOD and DCl were used. ReO FKC syn or ReO FGC anti (1.5−5.0 mg) was dissolved in 700 μL of a freshly prepared 0.01 M DCl in D_2O. The sample was transferred into a 5 mm NMR tube, and the pH of the solution was measured immediately and recorded. The proton NMR was measured at this pH, at 15 °C with a total number of eight scans. The number of scans was adjusted later as the sample concentration became diluted upon titration. After the first NMR measurement, the sample was titrated with NaOD (volume between 2 and 20 μL, concentration between 0.03 and 0.10 N). The pH and the volume of NaOD added were recorded only when the pH of the solution changed from 0.4 to 1 unit intervals, and then the sample was scanned on the Varian Inova 500 MHz NMR instrument at T = 288 K. We continued the titration and NMR measurements until pH 13.29 and, in the case of [ReO]FKC, reversed the titration adding DCl. Likewise, FKC and FGC ligands were also titrated using the above procedure.

Determination of pK_a. The technique used to determine pK_a's of the diastereomers and the tripeptide ligands is described in detail in the Supporting Information, and titration curves and fits are shown in Figures S4−S9.

Biodistribution Studies. Three tripeptides, FGC, FSC, and FKC, were chosen for radiolabeling with ^{99m}Tc and biodistribution studies in normal female nude mice. Samples of the individual ^{99m}Tc tripeptide diastereomers were isolated and evaluated for their biodistribution. Nude mice were injected with approximately 250−400 kBq of ^{99m}Tc-labeled compounds intravenously in the tail vein. Three mice per time point were sacrificed at 1, 4, and 24 h post injection for organ excision. Tissues collected included spleen, liver, kidney, lung, bone, heart, brain, fat (sample), thyroid, muscle (sample), skin (sample), blood (sample), tail, stomach, ovary, uterus, intestine, pancreas, and adrenals. Additionally, urine and feces were collected over time. The dissected tissues and collected excretions were counted for radioactivity in a γ counter (Compugamma LKB Wallac) and values of %ID/g and %ID were calculated and reported as a mean value together with standard deviation.

Results and Discussion

Chemistry. Choice of Tripeptide Sequences. Previous work on hydrophilic, unencumbered Tc and Re tripeptide complexes demonstrated that rapid interconversion of diastereomers precluded isolation and identification of the specific diastereomers.[9,24] Our goal was to identify common characteristics of diastereomers for all of the ^{99m}Tc tripeptide complexes (L amino acids with cysteine at the carboxylate terminus) and in this effort, assign the [^{99m}TcO]depreotide products as syn or anti. On the basis of prior literature and our observations that the $^{99m/99}$Tc depreotide diastereomers did not exhibit interconversion, we hypothesized that steric bulk, lypophilicity, and hydrogen-bonding opportunities of the amino acid residues inhibit the interconversion process. It was important to maintain the cysteine at the carboxylate terminus to mimic Tc depreotide and maintain the strong S−Tc/Re bond that stabilizes the complexes. So, by choosing the first two amino acids to have reasonably hydrophobic and sterically encumbered residues, we designed tripeptides that, when complexed to Tc or Re, exhibit minimal interconversion while maintaining water solubility and very closely mimicking ^{99m}Tc depreotide. Also, importantly, we discovered that acidic aqueous conditions and organic solvents minimized interconversion to allow isolation and crystallization.

Synthesis and Isolation of ^{99}Tc and Re Tripeptides. Treatment of $^{99}TcOCl_4^-$ and $ReOBr_4^-$ with tripeptides in methanol afforded the resulting [$^{99}Tc^{V}O$] and [$Re^{V}O$] diastereomeric complexes. Sodium acetate facilitated deprotonation of the two amide protons and the thiolate proton of the tripeptide. The complexation reaction proceeded swiftly, even in the absence of sodium acetate. The metal ions have a closed-shell d^2 electronic configuration and accept π electron density from the deprotonated amide and thiol groups. Deprotonated amide groups are common and expected in the reaction of peptides and peptide-like ligands with Tc(V)O and Re(V)O cores.[6,19,41,42] Several [TcO] and [ReO] tripeptide complexes were synthesized and their diastereomeric products isolated, including [TcO]FGC, [TcO]FKC, [TcO]MKC, [TcO]YKC, [TcO]YSC, [TcO]YDC, [TcO]YGC, [TcO](ϵK)GC, [ReO]FKC, and [ReO]FGC.

For both macroscopic [^{99}TcO] and [ReO], two major complexes, denoted A for the early eluting species and B for the later eluting species in reversed phase HPLC, were formed in an approximately 1:1 ratio for most of the tripeptide complexes. The exceptions were the FKC and YKC complexes, where B was favored (similar to [^{99m}TcO]-depreotide). Both species A and B were isolated for the metal complexes of each peptide, purified by semipreparative HPLC (method 3) and lyophilized to powders. For all of the rhenium complexes, powders arising from the lyophilization of both peak A and peak B products exhibited a peach color. However, for the ^{99}Tc complexes, the solutions and powders corresponding to peaks A and B were pink and yellow, respectively, in color. This striking color difference has been observed previously for other peptide-based Tc complexes.[24] The color profiles of [^{99}TcO]RP 290-bombesin peptide derivatives were also yellow and red. However, upon standing, the color of the separated fractions became identical over a period of 72 h at room temperature, a consequence of the interconversion process that resulted in approximately equal concentrations of the two ^{99}Tc diastereomers at equilibrium.[24]

We found that the use of organic solvents (i.e., limiting water) or acidic conditions minimized interconversion of the diasteromeric species. We also observed that interconversion is catalyzed in aqueous solution by base, vide infra. Hence, methanol was used for the preparation of the complexes, and

(41) Canney, D. J.; Billings, J.; Francesconi, L. C.; Guo, Y.-Z.; Haggerty, B. S.; Rheingold, A. L.; Kung, H. F. *J. Med. Chem.* **1993**, *36*, 1032−1040.
(42) Winnard, P.; Chang, P.; Rusckowski, M.; Mardirossian, G.; Hnatowich, D. J. *Nucl. Med. Biol.* **1997**, *24*, 425−432.

acidic conditions were used for the preparative HPLC. Thus, pure samples of fractions A and B of Tc and Re tripeptides were collected. In the case of FGC, the interconversion of B to an equilibrium mixture of A and B in slightly basic water was observed for Re and Tc. The conversion of B to A for [^{99}TcO]FGC was faster than that for [ReO]FGC, to an extent that we were not able to isolate enough of [^{99}TcO]-FGC peak B for physical characterization. To minimize interconversion during analytical measurements, NMR data was collected under acidic conditions or in organic solvents for selected samples, and CD data was collected in methanol. Inhibition of the interconversion of other non-peptide Tc^{V}O complexes and successful isolation of individual isomers by utilizing nonaqueous conditions has been reported previously.[13] Crystallizations of [TcO]FGC-product A, [ReO]-FGC-product A, [ReO]FGC-product B, [ReO]FKC-product B, and [TcO]YKC-product B were accomplished in organic solvents, and the crystals were checked by HPLC to verify the integrity of the compound.

The reaction of Na[TcO(ethyleneglycol)$_2$] with the peptide ϵ-benzoyl-Lys-Gly-Cys in methanol yielded two complexes that were isolated by prep HPLC; the complexes were not water soluble but were soluble in acetonitrile and slightly soluble in methanol. Crystallization of the yellow peak B was successfully accomplished from slow evaporation of an acetonitrile solution. Attempted crystallization of compound A (pink) did not yield X-ray quality crystals.

Infrared spectroscopy data were consistent with the formulations for the diastereomers (Supporting Information). The Re═O tripeptides showed a $\nu_{Re=O}$ stretch at 986 cm^{-1} and the Tc analogs showed a $\nu_{Tc=O}$ at 940 cm^{-1}, which are consistent with other Re(V)/Tc(V)═O square pyramidal, nitrogen−sulfur neutral complexes. HPLC retention times and IR data are given in Table S4 (Supporting Information).

Mass spectral data were consistent with the proposed structures of all of the MO tripeptide complexes but could not distinguish between the N1 amine (M^+) or N1 deprotonated amine ($[M + H]^+$) formulations (vide infra). For both the Tc and Re tripeptide diastereomers (Table S5), both a molecular ion $[M + H]^+$ and smaller peaks attributed to the sodium adducts $[M + Na]^+$ were detected. The Re analogs exhibit the characteristic Re isotopic pattern; Figure S3 shows the calculated and observed mass spectral data for the [ReO]-FKC analogs. For [ReO]FKC, both positive and negative electrospray data were collected. The $[M + H]^+$ peaks, the $[M - H]^-$ peaks, and the isotope patterns fit very well for the expected molecular ions of $ReC_{18}H_{26}N_5O_4S$. Interestingly, the syn diastereomer of [TcO](ϵ-K)GC appears to be a tightly associated dimer with $[M_2 + Na]^+$ at *m*/*z* 1065. This persists as the base peak even upon 10-fold dilution. The ions associated with the monomer are present at lower abundance. Low abundance peaks corresponding to the trimer are also present in a series beginning at *m*/*z* 1563 $[3(521) + 23]^+$.

Synthesis of Tracer ^{99m}Tc Complexes. The tracer ^{99m}Tc complexes were synthesized by the reduction of $^{99m}TcO_4^-$ with stannous ion in the presence of the tripeptide ligand and an exchange ligand (either tartrate or glucoheptonate). Analytical HPLC showed two peaks corresponding to the two diastereomers. Figure 4 shows the HPLC concordance experiment of $^{99m/99}$Tc FKC, where the tracer ^{99m}Tc peptide complexes coelute with the [^{99}TcO] peptide complexes, thus supporting the hypothesis that the structure and chemistry of the tracer are the same as those of the macroscopic compound under these conditions. Upon extended heating (30 min) of the kit at 100 °C, only the second peak (B) was present. Heating the kit at 100 °C for time periods less than 30 min resulted in a mixture of syn and anti diastereomers with mostly the peak B diastereomer. This result suggests that the species B that we identified as the syn diastereomer, vide infra, is more stable than the anti diastereomer.

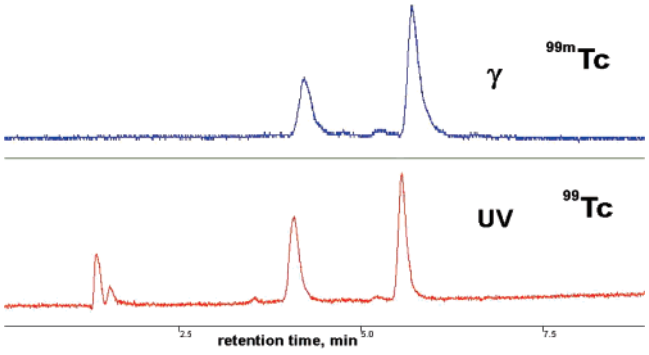

Figure 4. HPLC coelution studies of [$^{99/99m}$TcO]FKC. Top trace, γ detection of [^{99m}TcO]FKC (prepared using radiolabeling method 1 at room temperature); bottom trace, UV detection of [^{99}TcO]FKC. The coelution indicates that the same complexes are formed on the tracer and macroscopic levels.

X-ray Crystallography of Tc and Re Compounds. X-ray crystal structural characterizations of several tripeptide complexes ([TcO]FGC-product A, [ReO]FGC-product A, [ReO]FGC-product B, [ReO]FKC product-B, [TcO]ϵ-benzoyl-KGC-product B, and [TcO]YKC-product B) were performed. In all of the cases, the X-ray crystal structures showed that the early eluting peak (product A) corresponded to the anti diastereomer and the later eluting peak (B) corresponded to the syn diastereomer. These results combined with further characterization results (vide infra) led to the conclusion that product A for all of the [TcO]/[ReO] tripeptides corresponded to the anti diastereomer, whereas product B corresponded to the syn diastereomer. The samples did not interconvert during the crystallization process as verified by analytical HPLC taken on samples during crystallization as well as on the crystalline samples.

The crystal and structure refinement data for selected ^{99}Tc and Re tripeptide diastereomers ([ReO]FGC-syn and -anti, [TcO]FGC-anti, [ReO]FKC-syn, and [TcO]ϵ-benzoyl-KGC-syn) are given in Table S1, selected bond lengths and angles are listed in Table 1, and deviations of the amine and amide nitrogen atoms and the thiolate sulfur from the square plane constructed from these atoms are listed in Table 2. The crystal structure refinement data and bond lengths and angles for two additional complexes, [ReO]FKC-syn, crystallized from a basic aqueous solution, and TcO[YKC]-syn, crystallized from organic solution, are provided in Tables S2 and S3, in the Supporting Information. Ball and stick diagrams for selected crystal structures are given in Figure

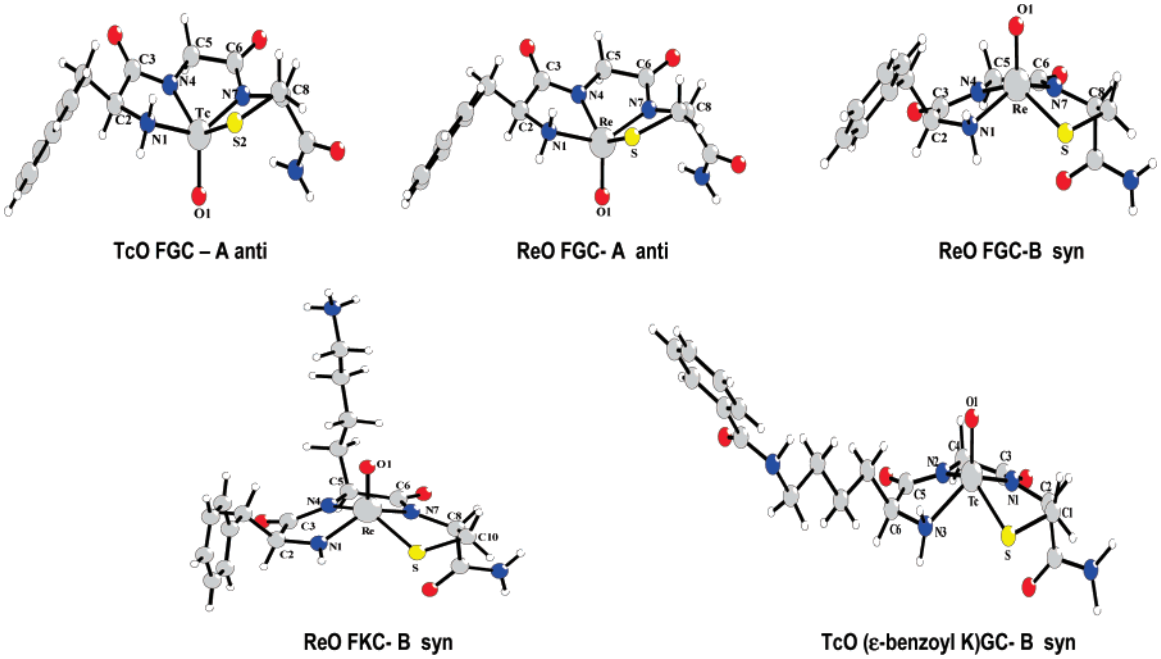

Figure 5. X-ray crystal structures for Tc and Re tripeptides in ball and stick representation.

5, and ORTEP diagrams for all of the species are presented in Figure S1.

The X-ray crystallography revealed two structural types that are mediated by a deprotonation process. The three complexes of the Phe-Gly-Cys (FGC) series and the [TcO]ϵ-benzoyl-KGC complex, all crystallized from organic solution, exhibit one type of structure where the N_1 (Figure on Table 1) of the first amino acid (phenylalanine or ϵ-benzoyllysine) is an amine nitrogen. In contrast, the X-Lys-Cys compounds ([ReO]FKC-syn crystallized from either organic solution or from basic aqueous solution, or [^{99}TcO]YKC-syn crystallized from organic solution) show a different solid-state structure wherein the N_1 of the phenylalanine or tyrosine is deprotonated and exhibits multiple bonding with the Re or ^{99}Tc, as evidenced by a shorter M$-$N$_1$ bond length (M = Tc, Re). Studies, described below, strongly suggest that in acidic and organic solution, the N_1 of [ReO]FKC and [TcO]YKC are in the amine form, vide infra.

Complexes of the first structural type (type 1), including [ReO]FGC-syn and -anti, [TcO]FGC-anti, and [TcO]ϵ-benzoyl-KGC-syn show typical bond lengths for the M$-$N$_{amine}$ (M$-$N$_1$, Table 2) that range from 2.111$-$2.129 Å, consistent with N$_{amine}$$-$M bond lengths from the literature, including the [ReO]RP290-syn complex and [ReO]RP294 ([ReO]-dimethylglycine-serine-cysteine).[9,19,41,43,44] The angles about the N$_{amine}$ atoms are close to tetrahedral at 109.5 degrees, consistent with a sp^3-hybridized nitrogen atom and a single bond to the metal atom. The M$-$N$_{amide}$ (M$-$N$_2$ and M$-$N$_3$, Table 1) bond lengths in the type 1 complexes are significantly less than the M$-$N$_{amine}$ bond lengths, as expected, ranging from 1.954 to 1.992 Å. These short bond lengths, along with angles about the N$_{amide}$ atoms of 117$-$122 degrees, suggest sp^2-hybridized nitrogen atoms and multiple bonding to the metal, consistent with the loss of the amide proton during complexation (also evidenced from NMR and mass spectral data; vide infra). The M$-$S$_{thiol}$ bond lengths ranged from 2.256 to 2.2828 Å, which is typical of M$-$S$_{thiol}$ bond lengths reported in the literature.[8,19,20,43,45$-$48]

The second crystalline type (type 2) was exhibited by compounds that possess lysine in the second position ([^{99}TcO]YKC-syn and [ReO]FKC-syn crystallized from organic or basic aqueous solution). In these structures, it was very clear that the M$-$N$_1$ bond was too short (1.931(9)$-$1.957 (7) Å) for a metal$-$amine bond. Instead, these bond lengths imply a stronger M$-$N bond, which would result from the N_1 amine deprotonation to form a metal$-$amide bond. The loss of a proton is further substantiated in the C$_4$$-N_1$$-$M bond angles about N_1 that approach 120 degrees, suggesting a sp^2-hybridized nitrogen. For the other type 2 complex M$-$N$_{amide}$ bonds (M$-$N$_2$ and M$-$N$_3$), the bond lengths are shorter (2.004, 2.005 Å) than a typical M$-$N$_{amine}$ bond but significantly longer than the M$-$N$_{amide}$ (M = ^{99}Tc,Re) bonds of type 1 complexes bearing the metal$-$amine bond at N_1. This lengthening of the N$_{amide}$$-$M bonds is consistent with a cis and trans effect initiated by the short N$_1$$-$M bonds. The bond angles around the amide N_2 and N_3 atoms (Table 2) are similar in the FKC and XGC series, all close to 120°, as expected for sp^2-hybridized nitrogen atoms.

(43) Francesconi, L. C.; Yang, Y. Y.; Kung, M.-P.; Xiao, X. Z.; Billings, J. J.; Guo, Y.-Z.; Kung, H. F. *J. Med. Chem.* **1994**, *37*, 3282$-$3288.
(44) Jurisson, S.; Schlemper, E. O.; Troutner, D. E.; Canning, L. R.; Nowotnik, D. P.; Neirinckx, R. D. *Inorg. Chem.* **1986**, *25*, 543$-$549.
(45) Edwards, D. S.; Cheesman, E. H.; Watson, M. W.; Maheu.L.J.; Nguyen, S. A.; Dimitre, L.; Nason, T.; Watson, A. D.; Walovitch, R. Neurolite and its metabolites. *Synthesis and Characterization of Technetium and Rhenium Complexes of N,N′-1,2-ethylenediylbis-L-cysteine*, 3rd ed.; Raven Press: New York, 1989.
(46) Mahmood, A.; Baidoo, K. E.; Lever, S. Z.; Nicolini, M.; Bandoli, G.; Mazzi, U., Eds. Cortina International Raven Press: Verona; 1989; Vol. *3*, pp 119$-$124.
(47) Melnik, M. *Coord. Chem. Rev.* **1987**, *77*, 275$-$324.
(48) Ohmomo, Y.; Franceconi, L. C.; Kung, M.; Kung, H. *J. Med. Chem.* **1992**, *35*, 157$-$162.

Table 3. Comparison of Cysteine α Proton and β Protons of [^{99}TcO] Tripeptides and [^{99}TcO]depreotide

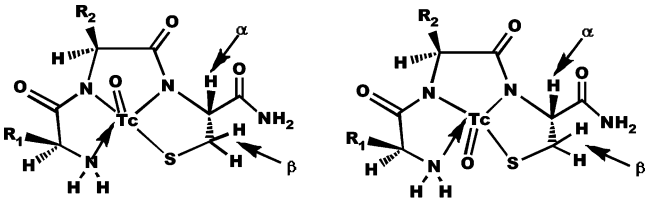

Syn Diastereomer

Anti Diastereomer

ANTI (Product A)	^{99}Tc Peptide	R_1	R_2	$\delta_{Cys\ \alpha}$-**H** (ppm)	$\delta_{Cys}\ \beta$-**H** (ppm)	J_{Cys} (Hz)
	^{99}Tc FGC	$-CH_2C_6H_5$	$-H$	5.58 (dd)	3.53, 3.71	$J_{H\alpha-H\beta1} = 7.8$, $J_{H\alpha-H\beta2} = 3.7$, $J_{H\beta1-H\beta2} = 12.3$
	^{99}Tc FKC	$-CH_2C_6H_5$	$-(CH_2)_4NH_2$	5.71 (dd)	3.57, 3.83	$J_{H\alpha-H\beta1} = 7.6$, $J_{H\alpha-H\beta2} = 2.2$, $J_{H\beta1-H\beta2} = 12.5$
	^{99}Tc MKC	$-CH_2CH_2SCH_3$	$-(CH_2)_4NH_2$	5.68 (dd)	3.56, 3.82	$J_{H\alpha-H\beta1} = 7.8$, $J_{H\alpha-H\beta2} = 2.0$, $J_{H\beta1-H\beta2} = 12.7$
	^{99}Tc YKC	$-CH_2C_6H_4OH$	$-(CH_2)_4NH_2$			
	^{99}Tc YSC	$-CH_2C_6H_4OH$	$-CH_2OH$	5.75 (dd)	3.56, 3.79	$J_{H\alpha-H\beta1} = 7.8$, $J_{H\alpha-H\beta2} = 2.4$, $J_{H\beta1-H\beta2} = 12.5$
	^{99}Tc YDC	$-CH_2C_6H_4OH$	$-CH_2COOH$	5.62 (dd)	3.57, 3.79	$J_{H\alpha-H\beta1} = 7.8$, $J_{H\alpha-H\beta2} = 3.4$, $J_{H\beta1-H\beta2} = 12.5$
	^{99}Tc YGC	$-CH_2C_6H_4OH$	$-H$	5.57 (dd)	3.48, 3.72	$J_{H\alpha-H\beta1} = 7.6$, $J_{H\alpha-H\beta2} = 3.7$, $J_{H\beta1-H\beta2} = 12.7$
	^{99}Tc depreotide	Figure 1	Figure 1	5.58 (dd)	3.36, 3.62	
SYN (Product B)	^{99}Tc Peptide	R_1	R_2	$\delta_{Cys\ \alpha}$-**H** (ppm)	$\delta_{Cys}\ \beta$-**H** (ppm)	J_{Cys} (Hz)
	^{99}Tc FGC	$-CH_2C_6H_5$	$-H$			
	^{99}Tc FKC	$-CH_2C_6H_5$	$-(CH_2)_4NH_2$	5.23 (d)	3.80	$J_{H\alpha-H\beta1} = 6.4$
	^{99}Tc MKC	$-CH_2CH_2SCH_3$	$-(CH_2)_4NH_2$	5.26 (dd)	3.87	$J_{H\alpha-H\beta1} = 5.4$, $J_{H\alpha-H\beta2} = 3.4$
	^{99}Tc YKC	$-CH_2C_6H_4OH$	$-(CH_2)_4NH_2$	5.25 (d)	3.83	$J_{H\alpha-H\beta1} = 6.6$
	^{99}Tc YSC	$-CH_2C_6H_4OH$	$-CH_2OH$	5.26 (dd)	3.84	$J_{H\alpha-H\beta1} = 6.6$, $J_{H\alpha-H\beta2} = 2.2$, $J_{H\beta1-H\beta2} = 12.7$
	^{99}Tc YDC	$-CH_2C_6H_4OH$	$-CH_2COOH$	5.25 (dd)	3.85	$J_{H\alpha-H\beta1} = 5.9$, $J_{H\alpha-H\beta2} = 3.9$
	^{99}Tc YGC	$CH_2C_6H_4OH$	$-H$			
	^{99}Tc depreotide	Figure 1	Figure 1	5.20 (d)	3.80	

The deprotonation in the type 2 complexes apparently renders the chelate ring slightly more planar as compared to that of the type 1 complexes. The deviations from a square plane formed by S, N1, N2, and N3 are slight for the FKC complexes compared to those of the FGC series (Table 2). The syn conformation for the later eluting peak B is preserved in the type 2 complexes.

Protonation Equilibria of the [TcO] and [ReO] Tripeptide Complexes. The chemistry of these systems can be understood by analysis of the crystallography data of all of the species along with their proton ^{1}H NMR data. Under acidic aqueous conditions (pH 3−4), all of the complexes of ^{99}Tc and Re tripeptides uniformly show very sharp proton NMR data, suggesting that one species is present and that no species exchange or interconversion is occurring.

All of the protons can be assigned in the NMR under acidic aqueous conditions except for the amine protons that are not observed (Supporting Information, Table S5). We attribute this to exchange of the amine protons in aqueous solution, which is a common occurrence known to be dependent on factors such as pH and concentration. The proton NMR data for [^{99}TcO] and [ReO]FKC and FGC complexes in organic solution (DMSO) show sharp, well-resolved proton resonances, consistent with a single species in solution, and furthermore, the amine protons (as well as all of the other expected protons in the metal complex) are clearly delineated (Supporting Information, Table S6 and Figure S2), indicating that the amine is protonated in a dilute organic solution. Our data is consistent with data from another NMR study in DMSO in which the two amine protons of a ^{99}TcO[Lys-Tyr-Cys] tripeptide complex were also observed.[49]

Despite the NMR evidence of the protonated amine species in organic solution, the deprotonated amine FKC and YKC complexes were crystallized from organic solutions. We postulate that deprotonation occurs as the concentration of the species increases upon evaporation. The driving force for the deprotonation may be the formation of a zwitterionic neutral species; in this case with an ϵ-NH_3^+ of the lysine

(49) Takayama, T.; Suzuki, K.; Sekine, T.; Kudo, H. *Radiochim. Acta* **2000**, *88*, 247−251.

Scheme 1. Equilibria between the Metal−Amine and the Metal−Amide Form of [ReO]FKC

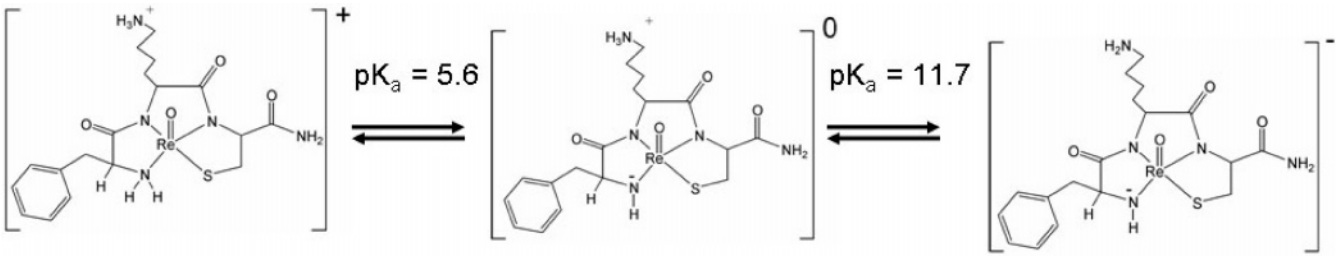

residue and the formal NH^- of the first amino acid (phenylalanine, tyrosine) bound to the M^VO. The deprotonation also occurred in basic solution as evidenced by the structural characterization results for the crystals isolated from a basic solution (Tables S1, S2, Figures 5, S1). The [ReO]FKC complex was very stable regarding pH extremes: in addition to the isolation of crystals at pH 13.3, we found that the complex remained intact in pH titrations from pH 1.7 to >12 and back to pH 1.7.

Potentiometric titrations and NMR titrations to assign pK_a values corroborate the deprotonation of the phenylalanine amine. Potentiometric titration of [ReO]FKC-syn showed a pK_a of 5.63 that corresponded to deprotonation of the phenylalanine amine (Scheme 1), as confirmed by NMR titrations monitoring chemical shifts of the β-H of the phenylalanine (Supporting Information, Figures S4−S6). The corresponding phenylalanine amine pK_a of the uncomplexed tripeptide, FKC, was 7.27; thus, as expected, the metal ion renders the amine proton substantially more acidic. The lysine residue also appears to profoundly increase the acidity of the phenylalanine amine proton compared to other tripeptides that do not contain lysine. The pK_a for [ReO]-FGC anti (6.80) was considerably higher than that for [ReO]-FKC-syn (5.63) (Figure S7). The pK_a for the phenylalanine amine of unbound tripeptide ligand FGC (7.43) was also higher than that for the FKC ligand (7.27). Titration studies revealed a further protonation equilibrium at pK_a = 11.7 for [ReO]FKC, which was assigned to the ϵ-NH_3 of the lysine side chain.

During the pH titration of [ReO]FKC-syn, we observed that precipitates formed in more concentrated solutions from pH 5 until 11. We attribute precipitation to the formation of a neutral species in aqueous solution. At pH below ~5, the syn diastereomer of [ReO]FKC is fully protonated and the positively charged species is water soluble. The amine of [ReO]FKC-syn deprotonates at pH ~5.6 to form a formally neutral species (i.e., a −1 N_{1amide} center with a +1 protonated lysine amine), and precipitation occurs. At pH above ~11.7, the diastereomer is further deprotonated at the epsilon-NH_3^+ moiety to form a negatively charged species that redissolves in aqueous solution, Scheme 1.

On the basis of these data, we can speculate on the pH product profile for [TcO]/[ReO] products possessing a lysine-containing amine diamide thiol N_3S chelator. At low pH (<5), the chelator amine is protonated and the metal chelator possesses a formally positive charge (a neutral metal center with a protonated, +1 lysine amine). At intermediate pH (including physiological pH), the deprotonated amine species with an overall neutral metal chelator predominates. At very high pH, a further proton is lost, and the metal chelator has a net negative charge (Scheme 1). Because [^{99m}TcO]-depreotide contains a Dap-Lys-Cys chelator, a similar equilibrium and species identity may be in effect in vivo for this radiopharmaceutical.

While attempting to measure the pK_a of the [ReO]FKC-anti diastereomer, we observed results that indicated that the deprotonated amine species mediates the interconversion process between the syn and anti forms. The NMR spectrum of [ReO]FKC-anti (Table S6, Supporting Information) did not change significantly from pH 2 to 4. However, upon increasing the pH above 4, the NMR spectrum resembled the spectrum of the syn analog and not the spectrum of the low pH anti species. Upon back-titration to low pH again with DCl, the NMR spectrum of the syn diastereomer persisted. Hence, it is likely that the deprotonation of the phenylalanine amine triggered the interconversion of the anti diastereomer to the syn diastereomer, which is more favored thermodynamically (as indicated by ^{99m}TcO radiolabeling and ^{99}Tc and Re macroscopic synthetic yield results). Once thermodynamic equilibrium was established, there was no tendency to re-form the anti isomer as the pH was lowered. This study implies that, at physiological pH, the syn diastereomer of ^{99m}Tc depreotide and ^{188}Re analogs persists in the zwitterionic form.

A comprehensive study by Hansen et al. indicates that a negatively charged carboxylate pendant group in the proximity of a secondary amine is responsible for a lower pK_a and deprotonation of the amine.[50] Further studies by this group showed that pK_a's of amines bound to Re^V=O are in the physiological range when pendant groups, such as carboxylate moieties, can bind to form a six-coordinate metal. They suggest that the acidity of amines is influenced by pendant groups, rigidity of the chelates, and the position of the C=O group within the chelate framework. In addition, the amine acidity was implicated to influence the syn−anti isomerization process. In our studies, the pendant lysine group in the FKC and YKC tripeptides appears to serve in a similar capacity, and we have further implicated the importance of the deprotonated amine in the interconversion process.

Spectroscopic Signatures of Syn and Anti [TcO]/[ReO] Tripeptide Diastereomers: NMR Spectroscopy. Several of the [^{99}TcO]/[ReO] tripeptide complexes, both syn and anti diastereomers, were analyzed by ^{1}H NMR. All of the protons

(50) Hansen, L.; Lipowska, M.; Melendez, E.; Xu, X.; Hirota, S.; Taylor, A. T.; Marzilli, L. G. *Inorg. Chem.* **1999**, *38*, 5351−5358.

for the [^{99}TcO] and [ReO] model peptides have been assigned and are presented in Table S6 in the Supporting Information. Close comparison of the results for the syn versus anti compounds led us to conclude that proton NMR spectra of the [^{99}TcO] complexes in acidic solution are diagnostic of the specific ^{99}Tc diastereomer.

The amide protons of the second amino acid and the cysteine were not observed by NMR, consistent with the loss of these protons on metal complexation. Protons on the three chelate rings formed upon complexation of the tripeptide with Tc and Re are shifted downfield as expected,[6] relative to those same protons on the free peptide. The chemical shifts and coupling constants are in agreement with previous reports of ^{99}Tc and/or Re tripeptides, although in those cases, the diastereomers had not been unambiguously assigned.[9,24,49] The NMR data for the first and second amino acids did not give much information about the diastereomer identification. However, the alpha (α) and beta (β) protons of the cysteine show distinct patterns in the [^{99}TcO] complexes that differentiate between the syn and anti diastereomers and are consistent with ^{99}Tc depreotide.

The chemical shifts for the α and β cysteine protons for Tc peptide diastereomers, tabulated in Table 3, reveal a unique signature. The α-proton resonances are significantly downfield shifted for anti diastereomers compared to syn diastereomers. Also, the β-proton resonances for anti diastereomers are split into a doublet or a doublet of doublets, whereas the syn diastereomers exhibit a single β-proton resonance. The chemical shifts and the splittings for the two diastereomers of [^{99}TcO]depreotide (also given in Table 3) are consistent with the tripeptide results and indeed allow for assignment of the syn and anti [TcO]depreotide products (details reported elsewhere).[23]

The distinction between syn and anti species by NMR is not as clear for the [ReO] analogs as for the [TcO] analogs. For the [ReO] tripeptides, the downfield shift of the anti diastereomer α protons is less pronounced than that for the Tc tripeptides, and two resonances are observed for the β-proton resonances for both diastereomers. The detailed chemical-shift assignments for the Re analogs, determined from the 2D experiments, for syn and anti diastereomers are given in Table S6 in the Supporting Information. Although some differences in the chemical shifts are noted between the cysteine protons of two pairs of diastereomers, more data would be required to conclude whether the Re tripeptide NMR results could discern between syn and anti species.

Spectroscopic Signatures of Syn and Anti [TcO]/[ReO] Tripeptide Diastereomers: Circular Dichroism Spectroscopy. The exact structures of both diastereomers for [ReO]-FGC were known unequivocally by X-ray diffraction experiments. CD spectra, recorded in methanol at 25 °C, of the anti and syn diastereomers of [ReO]FGC are shown in Figure 6 and tabulated in Table S7. The UV region below 300 nm gives information on the peptide backbone[51] and is not diagnostic for the syn and anti diastereomers. Both

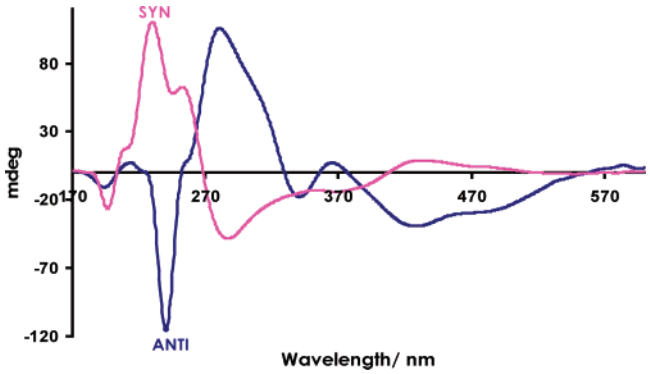

Figure 6. CD spectra of syn and anti ReO[FGC] diastereomers.

diastereomers exhibit small negative Cotton effects in the far-UV region (ca. 190 nm) indicating an absorption band due to $\pi \rightarrow \pi^*$ transitions from the peptide backbone. The positive and negative Cotton effects seen at around 230 nm, for the syn and anti diastereomers, respectively, are assigned to the n $\rightarrow \pi^*$ transition, due to the carbonyl group. A positive shoulder for the syn compound is observed at around 240 nm.

Transitions that involve the metal ion, such as ligand-to-metal charge transfer (LMCT) and ligand field transitions, occur in the region above 300 nm, and these transitions are, of course, the most revealing and important for the assignment of the metal complex diastereomers. A strong positive Cotton effect and a negative Cotton effect at around 300 nm, for the [ReO]FGC anti and syn diastereomers, respectively, are assigned to oxygen-to-rhenium charge-transfer transitions, according to a previous report for rhenium-Schiff base complexes.[52] The weak bands at lower energy in the visible region, at ca. 400 and 480 nm, likely result from LMCT transitions. The pronounced Cotton effects observed for the LMCT transitions demonstrate asymmetric induction from the enantiopure organic ligand to the metal center. The LMCT transition, which largely contributes to this region, dictates the structure and color of diastereomers. In the case of rhenium analogs, all of the complexes that we isolated were brown-red in color, consistent with the visible bands for both diastereomers having the same maxima in their absorbances. Hence, the [ReO]FGC results provided the first indications of different characteristic CD spectra for the syn and anti diastereiomers, and from there it was possible to compare the CD profiles of other diastereomers to the [ReO]-FGC spectra to look for features common to the individual diastereomer configurations.

CD spectra for several examples of the anti and syn diastereomers of [^{99}TcO] tripeptides, including [TcO](ϵK)-GC, [TcO]FGC, [TcO]FKC, [TcO]YSC, and [TcO]YDC taken in methanol at 25 °C are shown in Figure 7 along with results for ^{99}TcO[depreotide]. The ellipticities at different wavelengths for all of the species are tabulated in Table S7.

As observed for the [ReO] analogs, CD bands observed between 180 and 250 nm are attributed to transitions of the peptide backbone.[51] Examination of absorption and CD

(51) Cheng, Y.; Yan, Y.-B.; Liu, J. *J. Inorg. Biochem.* **2005**, *99*, 1952−1962.

(52) Bereau, V. M.; Khan, S. I.; Abu-Omar, M. M. *Inorg. Chem.* **2001**, *40*, 6767−6773.

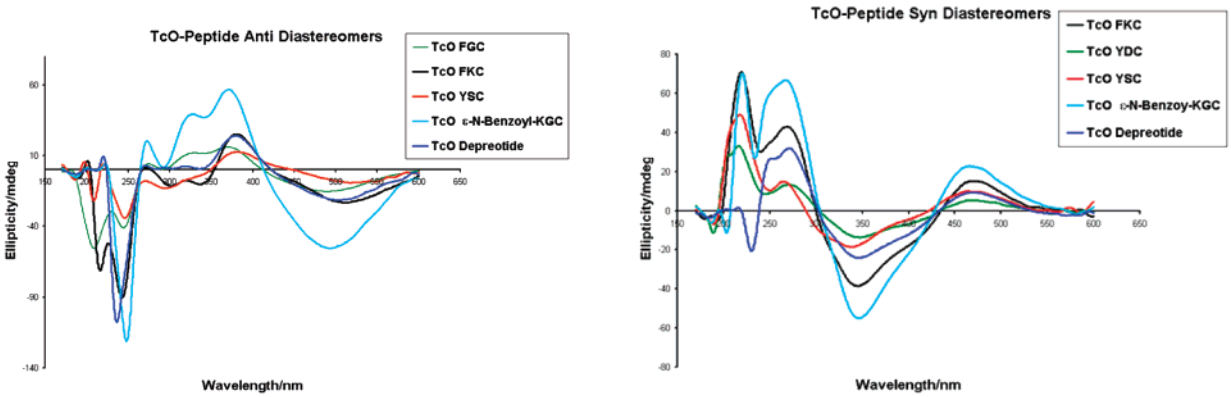

Figure 7. CD spectra of selected ^{99}Tc tripeptides and ^{99}Tc depreotide. Left: Isolated Products A from reverse phase HPLC postulated to be "anti" diastereomer. Right: Isolated Products B from reverse phase HPLC postulated to be the "syn" diastereomer.

spectroscopy of Tc thiolates from the literature suggests that the transitions found at ca. 400 nm are likely due to a thiolate-to-Tc(V) charge-transfer CT transition.[40,53] The bands at ca. 470 nm (syn diastereomers) and ca. 500 nm (anti diastereomers) are assigned to ligand field transitions, similar to spectral data of other characterized TcO^{3+} complexes possessing thiolate ligands and square pyramidal coordination.[53−55] The bands at ca. 350 nm may be higher energy ligand field bands or CT transitions.[53] The lowest energy ligand field band is centered at 500 nm for the anti diastereomers and centered at 460 nm for the syn diastereomers.

The transitions in the visible region report on the coordination of the Tc in the chelate, and thus the ellipticity patterns are diagnostic for the specific diastereomer (Figure 7). These transitions also give the [^{99}TcO] complexes their distinctive colors: the anti diastereomers are all pink and the syn diastereomers are all yellow. It is clearly seen that in the 300−600 nm region encompassing the LMCT and ligand field transitions, the CD patterns differ between the families of anti products (A) and syn products (B). The anti products all show bands with a positive Cotton effect between 300 and 400 nm and a broad asymmetrical band with a negative Cotton effect between 400 and 600 nm. All of the syn products show a broad asymmetrical band at 350 nm with a shoulder at around 400 nm, with a negative Cotton effect and a broad weak band with a positive Cotton effect centered at 460 nm. Thus, we observe characteristic CD signatures for the anti versus syn [TcO]/[ReO] metal centers, which should allow for unambiguous assignment of these diastereomers in radiopharmaceuticals that comprise peptide-based chelators, like [^{99m}TcO]depreotide and ^{188}Re P2045 (NeoTide).[23]

Biology. It was of interest to probe whether there are any inherent differences in biological behavior between the syn and the anti diastereomers of the metal tripeptide complexes. Therefore, three of the tripeptide ligands, FGC, FSC, and FKC, were radiolabeled with ^{99m}Tc, and the individual diastereomers were isolated by reverse phase preparative HPLC. By utililzing an ethanol/water HPLC mobile phase system, pH adjustment or evaporation steps on the collected fractions were not necessary (as they are with TFA/acetonitrile mobile phase systems) to make the injection solutions amenable for injection into animals; the samples were simply diluted with saline and injected into female nude mice. Animals were sacrificed at 1, 4, and 24 h, and biodistribution data was collected. Results for selected tissues are given in Table 4.

The biodistribution results show in general rapid clearance and accumulation of radioactivity mainly in the liver (1.3−4.9 %ID/g at 1 h post injection) and intestines (6.4−16.7 %ID/g at 1 h post injection). The FGC compound exhibited higher liver accumulation than FSC or FKC. These results attest to the relative lipophilicity of the model compounds. Some uptake in the kidneys (0.7−5.8 %ID/g) was also noted. Uptake in the thyroid is often indicative of free pertechnetate, and therefore can give a measure of the relative stability of the ^{99m}Tc complex. Although the absolute amounts of the three tracers in the thyroid are relatively low, it is clear that the FGC products gave significantly more thyroid uptake than the FSC or FKC products and therefore may be the least stable.

In comparing results between the diastereomers, it is apparent that the syn complexes show significantly higher uptake in several tissues, including kidney and lung (and liver at the early timepoint), as compared to the anti complexes. The syn complexes also exhibit substantially more radioactivity in the blood than the anti complexes. Taken together, these results might indicate that that the anti diastereomers would be preferred as imaging agents (less residual uptake in organs and better clearance). Certainly, if this trend persists with ^{188}Re, then tuning the amino acid residues to favor the anti diastereomer could be important. However, it should be emphasized that the biological distribution profile is driven by both the pharmacophore as well as the chelator, so one could not expect that using the anti chelator (especially on a larger biomolecule or peptide) would always lead to a better biodistribution profile.

(53) Jones, W. B.; Elgren, T. E.; Morelock, M. M.; Elder, R. C.; Wilcox, D. E. *Inorg. Chem.* **1994**, *33*, 5571−5578.
(54) Bryson, N.; Dewan, J. C.; Lister-James, J.; Jones, A. G.; Davison, A. *Inorg. Chem.* **1988**, *27*, 2154−2161.
(55) Franklin, K.; Howard-Lock, H.; Lock, C. *Inorg. Chem.* **1982**, *21*, 1941−1946.

Table 4. Biodistribution of ^{99m}TcO[F−X−C] (X = G, S, K) syn and anti Diastereomers in Female Nude Mice ($N = 3$)

%ID/g ± S.D.		1 h		4 h		24 h	
		anti	syn	anti	syn	anti	syn
lung	FGC	0.23 ± 0.02	1.41 ± 0.25	0.18 ± 0.01	0.85 ± 0.10	0.06 ± 0.02	0.12 ± 0.03
	FSC	0.31 ± 0.31	0.60 ± 0.09	0.08 ± 0.03	0.23 ± 0.07	0.03 ± 0.02	0.05 ± 0.01
	FKC	0.23 ± 0.04	0.42 ± 0.04	0.13 ± 0.01	0.09 ± 0.04	n.d.[a]	n.d.
kidney	FGC	1.52 ± 0.07	5.76 ± 1.78	1.11 ± 0.13	4.84 ± 1.15	0.56 ± 0.09	0.88 ± 0.07
	FSC	0.65 ± 0.11	2.91 ± 1.06	0.34 ± 0.04	0.80 ± 0.24	0.16 ± 0.04	0.23 ± 0.07
	FKC	1.37 ± 0.19	2.21 ± 0.41	0.44 ± 0.07	0.24 ± 0.05	n.d.	n.d.
liver	FGC	4.90 ± 0.54	3.75 ± 0.71	3.57 ± 0.13	2.00 ± 0.08	1.10 ± 0.18	0.54 ± 0.05
	FSC	1.26 ± 0.59	3.39 ± 0.62	0.95 ± 0.12	1.07 ± 0.61	0.35 ± 0.07	0.17 ± 0.03
	FKC	1.57 ± 0.62	4.30 ± 1.64	0.55 ± 0.09	0.96 ± 0.37	n.d.	n.d.
intestine	FGC	9.60 ± 0.91	10.4 ± 2.4	7.70 ± 1.84	11.1 ± 2.2	0.35 ± 0.21	0.21 ± 0.09
	FSC	15.7 ± 8.5	15.0 ± 4.1	9.29 ± 5.27	12.2 ± 4.3	0.15 ± 0.04	0.12 ± 0.08
	FKC	6.37 ± 0.71	11.8 ± 2.2	3.21 ± 0.74	10.8 ± 5.7	n.d.	n.d.
stomach	FGC	0.19 ± 0.07	1.42 ± 1.45	0.15 ± 0.07	1.44 ± 0.58	0.06 ± 0.02	0.17 ± 0.03
	FSC	0.25 ± 0.20	0.43 ± 0.27	0.37 ± 0.23	0.64 ± 0.78	0.06 ± 0.02	0.07 ± 0.03
	FKC	0.84 ± 0.28	0.73 ± 0.53	0.43 ± 0.04	0.34 ± 0.07	n.d.	n.d.
thyroid	FGC	0.53 ± 0.33	0.51 ± 0.18	0.48 ± 0.08	0.86 ± 0.31	0.28 ± 0.02	0.33 ± 0.04
	FSC	0.09 ± 0.02	0.19 ± 0.03	0.14 ± 0.03	0.20 ± 0.14	0.16 ± 0.05	0.24 ± 0.09
	FKC	0.19 ± 0.03	0.26 ± 0.04	0.07 ± 0.03	0.13 ± 0.04	n.d.	n.d.
pancreas	FGC	0.10 ± 0.02	0.24 ± 0.04	0.06 ± 0.02	0.17 ± 0.01	0.04 ± 0.01	0.07 ± 0.01
	FSC	0.19 ± 0.12	0.23 ± 0.15	0.03 ± 0.01	0.06 ± 0.02	0.02 ± 0.00	0.04 ± 0.01
	FKC	1.43 ± 0.45	2.52 ± 0.21	0.14 ± 0.02	0.12 ± 0.06	n.d.	n.d.
blood	FGC	0.35 ± 0.07	1.17 ± 0.16	0.20 ± 0.01	1.50 ± 0.06	0.06 ± 0.01	0.12 ± 0.02
	FSC	0.20 ± 0.02	0.45 ± 0.03	0.02 ± 0.00	0.36 ± 0.07	0.28 ± 0.02	0.03 ± 0.01
	FKC	0.16 ± 0.09	0.02 ± 0.00	0.04 ± 0.01	0.12 ± 0.03	n.d.	n.d.
muscle	FGC	0.01 ± 0.01		0.01 ± 0.00	0.02 ± 0.00	0.01 ± 0.00	0.01 ± 0.00
	FSC	not detectable	0.01 ± 0.00	not detectable	not detectable	not detectable	not detectable
	FKC	0.01 ± 0.00	0.01 ± 0.00	not detectable	n.d.	n.d.	n.d.
urine	FGC	62.5 ± 4.6	55.1 ± 4.2	60.6 ± 0.9	50.0 ± 7.4	51.8 ± 18.5	51.4 ± 5.3
	FSC	51.6 ± 5.3	45.3 ± 2.7	48.5 ± 9.4	44.7 ± 21.5	56.4 ± 6.4	55.5 ± 3.3
	FKC	74.1 ± 3.4	41.9 ± 7.2	54.8 ± 14.9	30.1 ± 8.7	n.d.	n.d.

[a] n.d. = not determined.

Conclusion

The assignment of the specific diastereomers for ^{99m}Tc or ^{188}Re radiopharmaceuticals is an important issue in radiopharmaceutical development. Crystallization and X-ray structural analysis, the best method to definitively identify the diastereomers, is generally untenable for intermediate size peptides becuase of multiple conformations. A good example of an intermediate size peptide radiopharmaceutical that has eluded X-ray structural analysis is [^{99m}TcO]depreotide. To investigate whether other methods of characterization might be able to define the structure of Tc depreotide, tripeptides that model the depreotide Tc binding site were synthesized and the [^{99}TcO] and [ReO] complexes were prepared. Interconversion was minimized by choosing amino acids whose residues were sterically bulky or possessed hydrogen-bonding capabilities. It was observed that basic conditions enhanced interconversion and that organic solvents (exclusion of water) minimized interconversion of the diastereomers.

Several [^{99}TcO] and [ReO] tripeptide syn and anti diastereomers were crystallized, the X-ray structures were determined, and the compounds were in addition characterized by proton NMR and CD experiments. The results indicated that the early eluting compound on reverse phase HPLC for both Tc and Re corresponds to the anti diastereomer, and the later eluting compound on reverse phase HPLC corresponds to the syn diastereomer. Furthermore, it appeared that proton NMR and/or CD spectroscopy results are diagnostic for the syn or anti configuration and therefore can be used to assign diastereomer identities to [^{99m}TcO]-depreotide or other similar ^{99m}Tc or ^{188}Re radiopharmaceuticals utilizing peptide-based chelators.

In addition, we have identified a deprotonation phenomena that occurs for [TcO]/[ReO] complexes of tripeptide chelators that comprise a lysine (e.g., FKC and YKC). For complexes of this type (including [TcO]depreotide), it appears that the deprotonated syn diastereomer is the predominant species in the physiological pH range. We also have obtained evidence that the deprotonated form may be an important intermediate in the syn-anti diastereomer interconversion process.

The biological behavior shows that the syn complexes had significantly higher uptake in several tissues, including kidney and lung (and liver at the early timepoint), as compared to the anti complexes. The syn complexes also exhibited substantially more radioactivity in the blood than the anti complexes. Ideally, rapid clearance from all tissues is desired and these data suggest that the anti conformation may be desired, especially for ^{188}Re if the ^{188}Re complexes behave similarly.

Along with the pharmacophore, the chelator portion dictates the biological distribution of a radiopharmaceutical.[56] Understanding the relationship between the structure and the biology is a key component in the design of targeted agents.

(56) Cyr, J. E.; Pearson, D. A.; Nelson, C. A.; Wilson, D. M.; Azure, M. T.; Zinn, K.; Dinkelborg, L. M.; Lister-James, J.; Dean, R. T. In *Technetium, Rhenium and other Metals in Chemistry and Nuclear Medicine 6*; Nicolini, M., Mazzi, U., Eds.; SG Editoriali-Italy: Padova, Italy, 2002; Vol. 6, pp 345−350.

With methods now in hand to identify diastereomers easily, we can begin to understand the features of amino acids that confer stability to specific diastereomers. We continue to investigate diasteromer stability due to the amino acid residues in proximity to the Tc and Re centers by theoretical and experimental means, and in the future, we hope to devise ways to design specific diastereomer structures of ^{99m}Tc and ^{188}Re tripeptide chelates that exhibit high in vivo stability by judicious choice of residues.

Acknowledgment. We gratefully acknowledge the following sources of support for this research: NSF grant CHE 0414218, NIH-S06 GM60654 (SCORE) (L.C.F.), the Faculty Research Award Program of the City University of New York (L.C.F.), and NSF grant MRI0116244 for the purchase of an X-ray Diffractometer (L.C.F.). Research Infrastructure at Hunter College is partially supported by NIH-Research Centers in Minority Institutions grant RR03037-08.

Supporting Information Available: NMR titrations monitoring chemical shifts, X-ray crystallographic files (CIF) for reported structures, and proton NMR data. This material is available free of charge via the Internet at http://pubs.acs.org.

IC070077P